Absolute optical oscillator strengths for the electronic excitation of atoms at high resolution: Experimental methods and measurements for helium

W. F. Chan, G. Cooper, and C. E. Brion
Department of Chemistry, The University of British Columbia, 2036 Main Mall, Vancouver, British Columbia, Canada V6T 1Z1
(Received 1 October 1990)

An alternative method is described for the measurement of absolute optical oscillator strengths (cross sections) for electronic excitation of free atoms and molecules throughout the discrete region of the valence-shell spectrum at high energy resolution (full width at half maximum of 0.048 eV). The technique, utilizing the virtual-photon field of a fast electron inelastically scattered at negligible momentum transfer, avoids many of the difficulties associated with the various direct optical techniques that have traditionally been used for absolute optical oscillator strength measurements. The method is also free of the bandwidth (line saturation) effects that can seriously limit the accuracy of photoabsorption cross-section measurements for discrete transitions of narrow linewidth obtained using the Beer-Lambert law $[I_0/I=\exp(nl\sigma_p)]$. Since the line-saturation effects are not widely appreciated and are only usually considered in the context of peak heights, a detailed analysis of this problem is presented, with consideration of the integrated cross section (oscillator strength) over the profile of each discrete peak. The suitability of the high-resolution dipole (e,e) method for general application to atomic and molecular electronic spectra is evaluated by test measurements of the absolute dipole (optical) oscillator strengths for the photoexcitation and photoionization of helium, since for this atom detailed quantum-mechanical calculations using highly correlated wave functions have been reported. The absolute scale is obtained from the Thomas-Reiche-Kuhn sum-rule normalization of the Bethe-Born transformed electron-energy-loss spectrum and does not involve the difficult determinations of photon flux or target density. The measured dipole oscillator strengths for helium excitation ($1\,^1S\rightarrow n\,^1P$, $n=2$–7) are in excellent quantitative agreement with the calculations reported by Schiff and Pekeris [Phys. Rev. **134**, A368 (1964)] and by Fernley, Taylor, and Seaton [J. Phys. B **20**, 6457 (1987)]. The absolute measurements are also compared with other experimental and theoretical oscillator strength determinations for photoexcitation and photoionization processes in helium up to 180 eV, including the $2snp$ and $3snp$ autoionizing resonances in the 59–72-eV energy region.

I. INTRODUCTION

A. General considerations

Absolute optical oscillator strength (cross section) information is of great importance because of the need to know electronic transition probabilities for both valence- and inner-shell excitation and ionization processes in many areas of application including plasmas, fusion research, lithography, aeronomy, astrophysics, space chemistry and physics, laser development, radiation biology, dosimetry, health physics, and radiation protection. Such information is also a crucial requirement for the development and evaluation of quantum-mechanical theoretical methods and for the modeling procedures used for various phenomena involving electronic transitions induced by energetic radiation.[1]

However, most spectroscopic studies to date for discrete electronic excitation processes have emphasized the determination of transition energies rather than oscillator strengths since the former quantities are generally relatively easier to obtain both experimentally and theoretically. In contrast, only rather limited information is available for the corresponding absolute optical oscillator strengths (or equivalent quantities reflecting transition probability such as cross section, lifetime, linewidth, extinction coefficient, A value) for atoms. In the case of discrete electronic transitions for molecules such quantities are extremely sparse, while for core (inner shell) processes the available data are even more limited. In particular oscillator strengths are in very short supply for transition energies beyond 10 eV where most valence-shell electronic excitation and ionization processes occur. This situation is partly due to the well-known inherent difficulties of quantitative work in the vacuum uv and soft-x-ray regions of the electromagnetic spectrum (i.e., beyond the LiF cutoff). These and other limitations provide considerable challenges in both photoabsorption and photoemission studies. The situation also reflects the limitations and application restrictions of other types of optical methods such as lifetime, line profile, self-absorption, and level crossing techniques.

From a theoretical standpoint, calculation offers an alternative approach to oscillator strength determination. However, such computational methods require extremely sophisticated correlated wave functions and reasonable accuracy is at present only feasible for the simplest atoms such as hydrogen[2] and helium.[3–9]

B. Optical methods for determining optical oscillator strengths for discrete transitions

A variety of different optically based methods have traditionally been used for the determination of most of the optical oscillator strength data available for discrete electronic transitions in the literature. Only a limited amount of data are available for atoms, and many of these are to be found in the important compilations published by Wiese and co-workers.[10] Very little information is available for molecules. The oscillator strength data base is extremely limited due to the fact that such measurements are difficult to perform and also because most available methods suffer from a variety of often serious difficulties and/or limitations which severely restrict their range of application. Wiese and co-workers[10] have discussed various aspects of the optical methods used for atoms and provides useful conversion formulas relating the various quantities produced by the different types of measurements.

The most commonly used optical measurement techniques include (a) photoabsorption via the Beer-Lambert law,[11] (b) lifetime measurements by level crossing techniques (including the Hanle effect),[12,13] (c) lifetime measurements by beam-foil methods,[14] (d) emission profile measurements from plasmas[15] and beams,[16] (e) resonance broadening emission profiles,[17] (f) self-absorption,[18–20] (g) total absorption,[21] and (h) optical phase matching.[22] The strengths and weaknesses of these methods with regard to their widespread general application to atomic and molecular spectra are summarized in Table I. Also shown in Table I are corresponding considerations for theory as well as for the electron-impact-based oscillator strength methods discussed in Sec. I C below. Methods (b)–(h) have all been used but only in selected favorable cases involving relatively intense atomic transitions. However, such approaches are generally complex and various limitations make them unsuitable for widespread application across the complete valence-shell spectral range for atomic and in particular molecular targets. Although in principle Beer-Lambert law photoabsorption measurements would seem to offer a straightforward means for routine measurement of absolute optical oscillator strengths for atomic and molecular transitions over a wide spectral range, application of the method may often result in large errors. Since the limitations of this method are not widely appreciated, the special case of the Beer-Lambert law photoabsorption method will now be discussed in detail.

C. Photoabsorption and the Beer-Lambert law

Photoabsorption via the Beer-Lambert law [method (a)] can in principle be applied readily to the complete valence-shell spectrum of atoms and molecules and the measurement procedure would seem to be quite straightforward in principle. However, in practice very few determinations of absolute oscillator strengths have actually been made using this method. This is because there are very serious problems that can arise when Beer-Lambert law photoabsorption spectra are used for absolute intensity (oscillator strength) determinations[23] rather than just for indicating energy levels. These problems, which are not always widely appreciated or well understood, arise from the finite energy resolution of any real optical monochromator.

The Beer-Lambert law can be stated as

$$\frac{I_0}{I}=\exp(nl\sigma_p)=\exp(N\sigma_p) \tag{1}$$

or

$$\sigma_p=\frac{1}{N}\ln\left[\frac{I_0}{I}\right], \tag{2}$$

where I_0 and I are the incident and transmitted light fluxes, respectively, n is the target density per cm^3, l is the path length in cm, σ_p is the photoabsorption cross section in cm^2 (1 Mb$=10^{-18}$ cm^2; 1 Mb$=1.0975\times10^{-2}$ differential oscillator strength units) and the column number $N=nl$. It should be noted, however, that Eqs. (1) and (2) are only strictly valid for the unphysical situation of zero bandwidth (i.e., infinite energy resolution) as discussed in Refs. 24–27. Difficulties arise because a logarithmic transform is required [Eq. (2)] in order to obtain the absolute cross section σ_p from the percentage transmission (I/I_0) obtained from the experimental measurements. As a result of this logarithmic transform the measured cross section at the characteristic energy will correspond to a weighted average cross section σ_p (which is often much less than the true cross section σ_p) in situations where the bandwidth (ΔE) is a significant fraction of, or greater than, the natural linewidth (ΔL) for a transition.[24–26] This limitation and the fact that measured peak values of cross sections are often a function of the instrument as much as of the target has been reviewed in some detail by Hudson[26] and commented on by others.[27,28] The situation is potentially particularly serious for intense narrow lines in the discrete region because of the Bohr frequency condition and the fact that the line profile varies rapidly within the bandwidth unless the latter is much narrower than the natural linewidth. Hudson[26] has also discussed the so-called "apparent pressure" effect and shown how the bandwidth effects can be minimized (but never entirely eliminated) by the tedious procedure of extrapolating measured peak intensities for each separate transition to zero column number N. However, even with such procedures, as Hudson[26] correctly points out, I approaches I_0 as this optically thin limit is approached and thus the greatest weight is placed on the least accurate data. The net result is that accurate optical oscillator strengths often cannot be obtained from photoabsorption measurements for very sharp, intense lines (for example, compare Refs. 11 and 29–33). These problems are likely to be particularly severe in the vacuum uv and soft x-ray regions of the spectrum where low light fluxes, even from monochromated synchrotron sources, often result in the use of wide monochromator exit slits. These bandwidth effects will occur when the usual arrangement exists with the monochromator placed between the continuum light source and the sample cell. This arrangement is the usual situation on synchrotron

TABLE I. Methods of obtaining optical oscillator strengths for discrete electronic transitions at high resolution.

Method (Ref.)	Advantages	Difficulties and problem areas	Suitability for general molecular studies
Beer-Lambert Law, photoabsorption (Ref. 11)	Simple relation, $I_0/I=\exp(nl\sigma p)$ Very high resolution Wide spectral range	Bandwidth effect (line saturation) due to the resonant nature of discrete excitation and use of logarithmic relation to obtain σ_p Stray light, order overlapping Extrapolation to zero column number	Limited suitability under favorable circumstances
Lifetime methods (Refs. 12–14)	No bandwidth problem	Branching ratios must be known Molecular energy states must be known	Not generally suitable
(i) Level crossing (Hanle effect) (Refs. 12 and 13)	Good for strong resonances	Slight dependence of linewidth on background pressure	
(ii) Beam foil (Ref. 14)	Useful for mean lifetimes of excited state atomic and ionic levels	Cascades from other states Blending of unresolved spectral lines	
Plasma emission profile (Ref. 15)	No bandwidth problem	Only good for optically thick emission Uncertainties in calculated Stark width	Difficult and not generally suitable
Beam emission profile (Ref. 16)	No bandwidth problem	Time variations in Doppler width Relies on calculated electron collision cross section	Difficult and not generally suitable
Resonance broadening emission profile (Ref. 17)	No bandwidth problem	Extrapolation to zero pressure Different Doppler width corresponding to different excitation to upper levels.	Difficult and not generally suitable
Self-absorption (Refs. 18–20)	No bandwidth problem	Possible departure from Doppler profile Re-emission from atoms excited by absorption of resonance photons	Difficult and not generally suitable
Total absorption (Ref. 21)	No bandwidth problem	Only good for optically thick absorption in the absence of collision broadening	Difficult and not generally suitable

TABLE I. (*Continued*).

Method (Ref.)	Advantages	Difficulties and problem areas	Suitability for general molecular studies
Optical phase matching (Ref. 22)	No bandwidth problem	Transition peak must not be perturbed by collision effects Refractive index of buffer gas at particular wavelength must be known	Difficult and not generally suitable
Electron scattering (vary θ at fixed E_0) (Refs. 38 and 41)	No bandwidth problem	Extrapolation to $K^2=0$ is problematic Tedious procedure for each transition Absolute scale requires external procedures	Difficult but possible
Electron scattering (vary E_0 at fixed θ) (Ref. 42)	No bandwidth problem	Extrapolation to $K^2=0$ is problematic Tedious procedure for each transition Electron optical effects and lens ratio Absolute scale requires external procedures	Difficult for general application
Electron scattering	No bandwidth problem	Stray electrons	Readily applicable over wide spectral range
HR Dipole (e,e) (this work)	Absolute scale via TRK sum rule No pressure or incident flux measurements required Direct Measurement over wide spectral range Good accuracy	Accuracy of Bethe-Born conversion factor since $B(E)$ in low-energy region is dependent on extrapolation Resolution limited to $\Delta E \geq 0.01$	Most difficulties can be overcome with very careful experiments
Quantum-mechanical calculation (Refs. 3–9)	Very accurate for small atoms No instrumental effects Infinite energy resolution	Extension to large systems limited by wave-function accuracy and calculation methods Lack of sufficiently accurate experimental data for comparison	Very difficult to obtain good accuracy

beam lines (i) because of the ultrahigh vacuum requirements in the storage ring and the monochromator and (ii) because the monochromator is usually an integral part of the beam line facility feeding different possible experimental arrangements. However, these spurious bandwidth effects would also influence the measured cross-sections if the sample cell was placed between the source and monochromator as occurs in many laboratory spectrometer arrangements.

Despite the serious deficiencies which can complicate the determination of absolute optical oscillator strengths for discrete transitions using the Beer-Lambert law, it is still sometimes used and it can then often result in spurious results which are not always apparently realized by the experimenters. A particularly drastic example of such "line-saturation" bandwidth effects occurs in the vacuum uv absorption spectrum of N_2 (Ref. 33) illustrated in Fig. 1. The vacuum uv spectrum as reported by Gürtler, Saile, and Koch[33] on an absolute scale [Fig. 1(a)] has high enough resolution to show evidence of rotational effects. This optical absorption spectrum[33] is compared with a high impact energy, negligible momentum transfer, high-resolution ($\Delta E = 0.017$ eV) electron-energy-loss spectrum[34] in Fig. 1(b) over the same energy region. Clearly three are large differences in relative intensity, in the 12.6–13.0-eV range and particularly in the 12.9–13.0-eV region. These differences reflect serious line-saturation effects in the optical work in the 12.9–13.0-eV region due to the finite bandwidth of the incident radiation and the extremely narrow natural linewidth of these intense transitions. As can be seen from Fig. 1 these factors have dramatic effects on the derived optical oscillator strength (cross section) in the photoabsorption spectrum. Clearly not only the peak height but also the peak area (and thus the apparent oscillator strength) is drastically reduced in the optical spectrum. In contrast, the corresponding absolute optical oscillator strength spectrum obtained via electron-energy-loss spectroscopy (EELS) in Fig. 1(b) (see Sec. I D) shows the correct relative intensities (band areas) even though it is at lower energy resolution than the optical work. This large intensity effect in the electronic spectrum of N_2 was earlier pointed out in electron impact studies by Lassettre *et al.*[35] and also by Geiger and Stickel.[36] Subsequently, extrapolation of very carefully controlled optical measurements,[31,32] made as a function of column number N, was found to give results consistent with the intensities derived from the EELS measurements.[35,36]

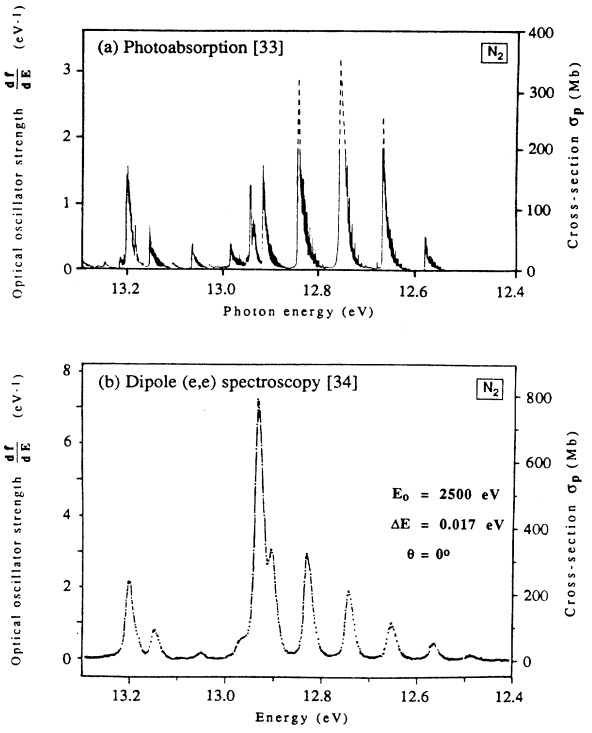

FIG. 1. Comparison of the valence-shell electronic excitation spectra of nitrogen obtained by photoabsorption and electron-impact experiments in the energy region 12.4–13.2 eV. (a) Absolute photoabsorption spectrum adapted from Fig. 1 of Ref. 33—the dashed lines have been drawn to show the position of the maximum cross sections of the peaks according to the numerical values given in the text of Ref. 33. (b) Electron-energy-loss spectrum (Ref. 34)—the spectrum was made absolute by reference to a recently obtained oscillator strength spectrum of N_2 (Ref. 86).

It is important to note that the treatment of line-saturation effects by Hudson[26] only emphasizes the effects of finite bandwidth on the *peak heights* of sharp spectral lines (i.e., the cross section at the maximum) and how such effects may, hopefully, be minimized by extrapolation to zero column number. As Hudson[26] has shown, a 40% error still exists in a peak *height* cross section for the situation where the linewidth and bandwidth are equal, even at $N = 0$. However, it should be remembered that an accurately measured oscillator strength for a discrete transition should involve an integral over the whole profile of the spectral line and should not just be assessed from the peak height. The peak area in a photoabsorption experiment is of course also severely influenced by the bandwidth effects, which result in a significant reduction in both peak height and peak area, as can be seen in Fig. 1. This clearly leads to an integrated optical oscillator strength for the transition which is significantly in error unless the bandwidth is very narrow compared with the narrowest features in the spectrum—regardless of whether or not such features are resolved. Such errors are therefore likely to be particularly serious for molecular spectra because of the vibrational and rotational fine structure—as can be seen in Fig. 1. Since in general different lines in the same spectrum have different natural linewidth the cross-section perturbations are furthermore different for every transition [see again Figs. 1(a) and 1(b)]. Thus the complete spectroscopy (i.e., all linewidths and line shapes) must already be known if any meaningful understanding of photoabsorption cross sections for spectral lines is to be obtained. If such information were available, then of course the oscillator strengths would already be known from the linewidths. Clearly then, one can never be sure that the correct oscillator strength has been obtained in a photoabsorption experiment unless either the information is already available in some form from other sources, or the absolute integrated

spectral intensities can be shown to be effectively independent of the bandwidth as well as the column number N.

Given the above considerations it is necessary to extend the peak height analysis of Hudson[26] to consider the effects of bandwidth on the integrated cross section over the spectral line profile (i.e., *peak area)* in the photoabsorption experiment. For example, consider (Fig. 2) the effects of convoluting an assumed Gaussian-shaped absorption peak of natural linewidth ΔL with a triangular monochromator bandwidth ΔE. In this case, Eq. (1) can be rewritten as

$$I(\Delta E,E)=I_0(\Delta E,E)\exp[-(\sigma_p(\Delta E,E)N] \ . \tag{3}$$

The area A_1 (see Fig. 2, left-hand side) of the unconvoluted Gaussian absorption peak depends linearly on the percentage absorption $[(I_0-I)/I_0]$ of $I_0(E)$ at the peak maximum for a given ΔL. The area of the Gaussian peak is, of course, unchanged by convolution with the bandwidth ΔE regardless of $\Delta E/\Delta L$. That is, considering the percentage absorption

$$\int^{\text{peak}} \frac{I_0(E)-I(E)}{I_0(E)}dE=\int^{\text{peak}} \frac{I_0(\Delta E,E)-I(\Delta E,E)}{I_0(\Delta E,E)}dE , \tag{4}$$

or

$$A_1=A_2 \ .$$

However, in order to calculate the photoabsorption cross section $\sigma_p(E)$ a logarithmic transformation [see Eq. (2)] of I_0/I is needed. The logarithmic transform, together with the resonant nature of discrete excitation by photons, is the root cause of the line-saturation bandwidth effects and the resulting spurious experimental cross sections which often occur in absolute photoabsorption measurements using Beer's law. In the case of the logarithmic conversion we have for the cross-sectional areas before and after convolution (Fig. 2, right-hand side)

$$A_3=\int^{\text{peak}}\sigma_p(E)dE=\frac{1}{N}\int^{\text{peak}}\ln\frac{I_0(E)}{I(E)}dE \ , \tag{5}$$

$$A_4=\int^{\text{peak}}\sigma_p(\Delta E,E)dE=\frac{1}{N}\int^{\text{peak}}\ln\frac{I_0(\Delta E,E)}{I(\Delta E,E)}dE \ . \tag{6}$$

It is found that A_3 is always greater than A_4 unless ΔE is equal to zero, which is only true of course for the hypothetical case of infinitely narrow bandwidth. In more detail mathematically, area A_1 is convoluted by bandwidth ΔE to yield an area A_2 such that $A_1=A_2$. If area A_2 is also a Gaussian distribution with full width at half maximum (FWHM) approximately equal to $(\Delta L^2+\Delta E^2)^{1/2}$, then under this circumstance, $A_1=A_2$ $(=1/S)$ (where S is a scale factor in order that we may vary the area under the Gaussian peak). After integration of Eqs. (5) and (6), we obtain

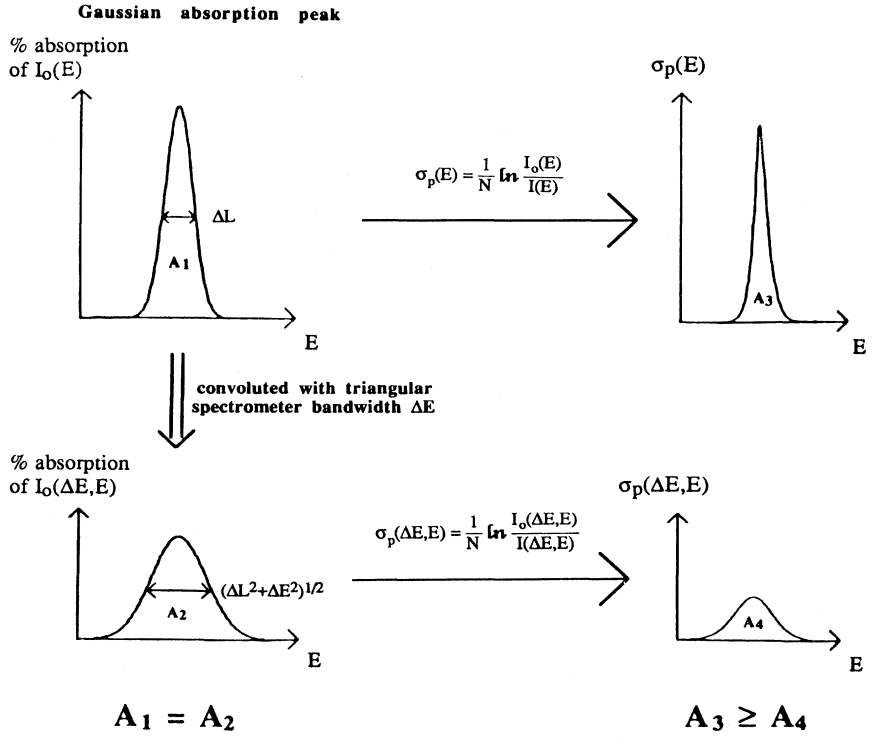

FIG. 2. Diagrammatic representation of the line-saturation effect occurring in photoabsorption experiments when the Beer-Lambert law is used to determine the integrated cross section of a discrete transition.

$$A_3=\frac{1}{N}\left[\sum_{n=1}^{\infty}\frac{C_1^{n-1}}{\Delta L^{n-1}S^n n^{1/n}}\right], \tag{7}$$

$$A_4=\frac{1}{N}\left[\sum_{n=1}^{\infty}\frac{C_1^{n-1}}{[(\Delta L^2+\Delta E^2)^{1/2}]^{n-1}S^n n^{1/n}}\right], \tag{8}$$

where

$$C_1=\frac{2\sqrt{\ln 2}}{\sqrt{\pi}}.$$

Comparing each term for Eqs. (7) and (8), A_3 is always greater than A_4 unless ΔE is zero, and only in this case does $A_3=A_4$.

In Fig. 3, the variation of observed peak area (NA_4) with column number N for a given transition is shown for different $\Delta E/\Delta L$ ratios. It shows that the area becomes smaller with an increase in the ratio $\Delta E/\Delta L$ for the same column number. Figure 4 shows the variation of integrated cross section for a given transition obtained by use of the Beer-Lambert law with column number for different values of $\Delta E/\Delta L$. The true integrated cross section (100 Mb eV) is only attained at $N=0$ or where $\Delta E=0$ (i.e., infinite resolution). Figures 5(a)–5(e) show the variation of observed integrated cross sections with column number at $\Delta E/\Delta L=10$, calculated for a series of transitions of different true cross sections (given at zero column number). Note that for each cross section the behavior is different even for a fixed ΔL. Since in general different lines will have different natural linewidths ΔL, it can be seen that the effects and therefore the interpretation of photoabsorption experiments can be very complex indeed. These effects are known as the line-saturation or apparent pressure effects occurring in photoabsorption experiments.[26] With a very narrow natural linewidth (i.e., large $\Delta E/\Delta L$) and a high cross section the problem is obviously more severe. In order to attempt to obtain a result closer to the correct cross section, the only experimental approach is the tedious procedure of performing

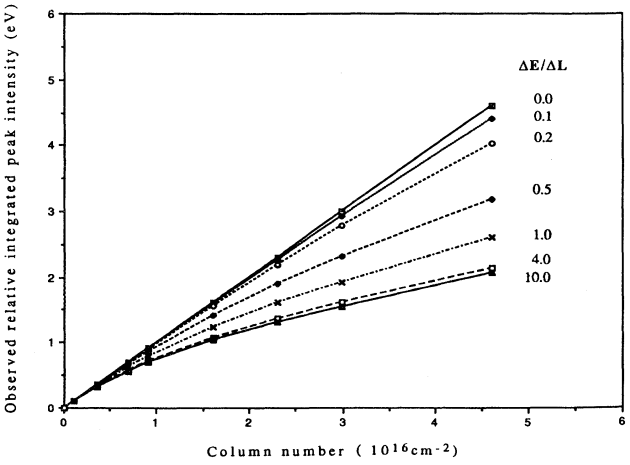

FIG. 3. Variation of integrated peak intensity (NA_4) with column number for different ratios of $\Delta E/\Delta L$ (incident bandwidth to natural absorption linewidth ratio), calculated using Eqs. (7) and (8).

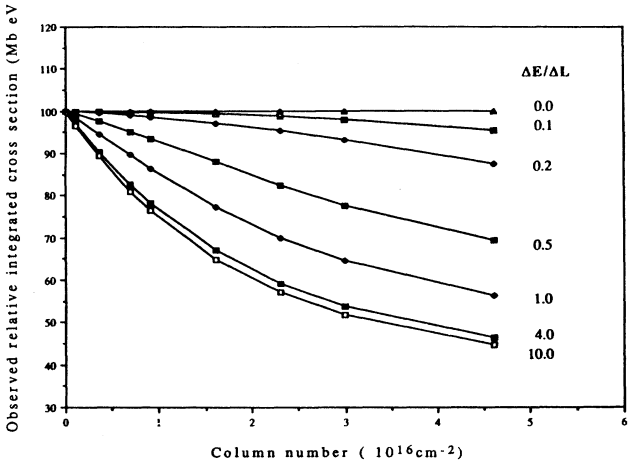

FIG. 4. Variation of the observed integrated cross section with column number for different $\Delta E/\Delta L$ ratios, calculated using Eqs. (7) and (8). The true integrated cross section is taken to be 100 Mb eV.

the measurements for each transition in the spectrum at a series of pressures and extrapolating to zero column number as shown in Figs. 4 and 5. Such procedures have been used by Lawrence, Mickey, and Dressler,[31] and by Carter.[32] In Fig. 5 we can see that for peaks with the same $\Delta E/\Delta L$ value, the higher the true cross section, the greater the error in the optically measured cross section at a given column number. Thus it can be seen that for very narrow peaks of very high cross section, extrapolation to extremely low pressure would be required one to obtain the correct cross section experimentally. However, in an actual experiment, the error in measuring $I_0(\Delta E,E)/I(\Delta E,E)$ increases with decrease in pressure. As Hudson[26] has pointed out, extrapolation procedures

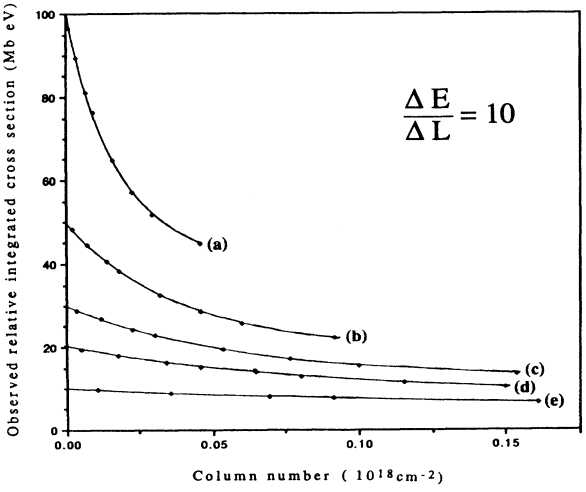

FIG. 5. Variation of the observed integrated cross section with column number at $\Delta E/\Delta L=10$ for peaks with true integrated cross section of (a) 100, (b) 50, (c) 30, (d) 20, and (e) 10 Mb eV. The curves were calculated using Eqs. (7) and (8).

put the most emphasis on the least-accurate data and hence the extrapolated value is likely to be inaccurate. The procedure only minimizes the bandwidth effect and the resulting cross section may in some cases still be subject to large error. As one example, Yoshino *et al.*[11] have stated that the (12,0) transition of $^{18}O_2$ is too narrow to be measured using the Beer-Lambert law photoabsorption method.

In summary then, the above model calculations indicate that it is often extremely difficult to obtain highly accurate optical oscillator strengths for discrete transitions in optical photoabsorption experiments based on the Beer-Lambert law, especially for very sharp peaks with high cross section. As such, absolute photoabsorption cross sections obtained for discrete transitions using the Beer-Lambert law must always be viewed with some caution because of the possibility of significant systematic errors due to finite bandwidth effects, which in general will be different for every transition. Therefore widespread application of Beer-Lambert law photoabsorption methods to the study of discrete atomic and molecular spectra is not practical if accurate cross sections are desired. In the following discussion alternative methods of determining optical oscillator strengths are described that do not suffer from these spurious bandwidth effects.

D. Electron-impact methods for determining optical oscillator strengths

An alternative and entirely independent approach to optical oscillator strength determination, free of spurious bandwidth effects, is provided by exploiting the virtual-photon field-induced in a target by fast electrons. This can be utilized by means of fast electron-impact electron-energy-loss techniques at vanishingly small momentum transfer. The theoretical relation between high-energy electron scattering and optical excitation has long been understood.[37] The resonant process of absorption of a photon of energy E

$$h\nu(E)+M\rightarrow M^* \tag{9}$$

may be compared with the nonresonant process of electron-impact excitation

$$e(E_0)+M\rightarrow M^*+e(E_0-E)\ . \tag{10}$$

Clearly the electron-energy loss (E) is analogous to the photon energy E. The intensity of scattered electrons is measured rather than a percentage absorption. The nonresonant nature of the electron-impact excitation process together with avoidance of the logarithmic Beer-Lambert law in determining oscillator strength (cross section) means that the line-saturation bandwidth problem, which often complicates photoabsorption experiments, is eliminated in the EELS method.[27]

It is useful to review some aspects of the theory of inelastic scattering of fast electrons. A key quantity in the electron-impact method for determining optical oscillator strength is the momentum transfer ($\mathbf{K}$) in the collision. A momentum-transfer-dependent, differential generalized oscillator strength $df(\mathbf{K},E)/dE$, describing the transition probability, can be defined and it is related[27] to the differential inelastic electron-impact cross section $d^2\sigma_e(\mathbf{K},E)/dEd\Omega$ for discrete transitions by the equation

$$\frac{df(\mathbf{K},E)}{dE}=\left[\frac{E}{2}\frac{\mathbf{k}_0}{\mathbf{k}_n}\mathbf{K}^2\right]\frac{d^2\sigma_e(\mathbf{K},E)}{dEd\Omega}\ , \tag{11}$$

where E is the energy loss and $\mathbf{k}_0$ and $\mathbf{k}_n$ are the incident and scattered momenta respectively. $d^2\sigma_e(\mathbf{K},E)/dEd\Omega$ as a function of energy loss E is the electron-energy-loss spectrum at momentum transfer $\mathbf{K}$ involving scattering into a solid angle element $d\Omega$. The various momenta are related to the polar scattering angle θ by the cosine rule

$$\mathbf{K}^2=\mathbf{k}_0^2+\mathbf{k}_n^2-2\mathbf{k}_0\mathbf{k}_n\cos\theta\ . \tag{12}$$

According to the Bethe-Born theory[37]

$$\frac{df(\mathbf{K},E)}{dE}=\frac{df^0(E)}{dE}+A\mathbf{K}^2+B\mathbf{K}^4+\cdots\ , \tag{13}$$

where $df^0(E)/dE$ is the differential optical oscillator strength and A, B, etc. are constants. Therefore, at the so-called optical limit, which corresponds to zero momentum transfer,[27]

$$\lim_{\mathbf{K}^2\rightarrow 0}\frac{df(\mathbf{K},E)}{dE}=\frac{df^0(E)}{dE}\ . \tag{14}$$

Under such conditions of negligible momentum-transfer dipole selection rules apply and

$$\frac{df^0(E)}{dE}=\left[\frac{E}{2}\frac{\mathbf{k}_0}{\mathbf{k}_n}\mathbf{K}^2\right]\frac{d^2\sigma_e(E)}{dEd\Omega}=B(E)\frac{d^2\sigma_e(E)}{dEd\Omega}\ . \tag{15}$$

The quantity $B(E)$ is called the Bethe-Born factor and it can be seen that it depends on kinematic (i.e., instrumental) factors alone. In an actual experiment the factor $B(E)$ must also take into account the finite acceptance angles about the mean scattering angle of 0°. This will be considered in Sec. II below. $B(E)$ relates the electron-impact differential cross section at negligible momentum transfer to the differential optical oscillator strength. It is clear from Eqs. (11)–(15) that electron-impact measurements under appropriate conditions may be used to make absolute optical measurements if appropriate absolute normalization procedures can be established. The momentum transfer $\mathbf{K}$ depends on the impact energy E_0 and the mean scattering angle θ [see Eq. (11)]. In particular $\mathbf{K}^2\rightarrow 0$ at $E_0\gg E$ and $\theta\rightarrow 0°$ and this leads to two general approaches which have been used for optical oscillator strength determination by electron impact.

(i) An indirect EELS method, pioneered in the 1960s by Lassettre and co-workers,[38–41] involves measurement of the relative intensity for a given transition as a function of scattering angle (i.e., of $\mathbf{K}^2$) at a fixed intermediate impact energy (typically ~ 500 eV). This results in a relative generalized oscillator strength curve [see Eqs. (12)–(14)], which can be extrapolated to $\mathbf{K}^2=0$ to give an estimate of the relative optical oscillator strength for the transition. The extrapolation procedure is tedious since a series of measurements is required for each transition. In addition, the procedure can often be problematic due to unusual behavior of the functional form of $f(\mathbf{K})$ at low $\mathbf{K}$ (Ref. 41) and also due to the fact that the minimum ex-

perimental value of $\mathbf{K}^2$ was often quite large,[38–41] so that a lengthy extrapolation was involved. The minimum attainable value of $\mathbf{K}^2$ was further limited[38–41] by the fact that the spectrometer could not be operated at $\theta=0°$ due to interference from the incident primary electron beam in the electron-energy-loss analyzer. The relative value of the oscillator strength is usually made absolute by reference to concurrent measurements of the relative elastic-scattering intensity, which is in turn normalized on a published value of the calculated or experimental absolute elastic-scattering cross section. A variation of this extrapolation approach, used by Hertel and Ross to study alkali metals,[42] involved scanning the impact energy at fixed scattering angle for each transition. However, such an approach is even more difficult for general application to quantitative work because of electron optical effects on the scattered electron intensities, and therefore its use has been extremely limited.

(ii) A more direct and versatile approach, which avoids the need for the undesirable extrapolation procedures, is to choose the experimental conditions so that the optical limit (i.e., $\mathbf{K}^2\rightarrow 0$) is effectively satisfied directly.[43–45] This can be achieved by measuring at high impact energy E_0 (typically 3000 eV for valence-shell processes) and designing the electron analyzer and associated electron optics so that a mean scattering angle of 0° can be used.[46–50] This results in $\mathbf{K}^2<10^{-2}$ a.u. Under such conditions Eq. (15) is satisfied to better than 1% accuracy and an entire EELS spectrum covering both the discrete and continuum regions can be obtained directly under dipole (optical) conditions. To obtain the relative optical oscillator strength spectrum it suffices merely to transform the relative electron-impact differential cross section (at $\mathbf{K}^2\sim 0$) by the known Bethe-Born factor $B(E)$ for the spectrometer. $B(E)$ must take into account the effects caused by the finite acceptance angles of the electron-energy-loss analyzer (i.e., a spread of $\mathbf{K}^2$). The relative optical oscillator strength spectrum obtained in this way has the correct relative intensity distribution because of the "flat" nature of the virtual-photon field[51,52] associated with inelastically scattered fast electrons at $\mathbf{K}^2\sim 0$.[37] This means that no determination of beam flux is required. The relative spectrum can be made absolute by using a known theoretical[47] or experimental[49] value of the photoabsorption cross section at a single photon energy, usually in the photoionization continuum. However, an independent and accurate means of obtaining an absolute scale, frequently used in this laboratory (for some examples see Refs. 53–55) is to obtain the Bethe-Born transformed valence-shell EELS spectrum [i.e., $d^2\sigma_e(E)/dE\,d\Omega$—see Eq. (15)] out to high energy loss. The total area of the spectrum is then normalized to the number of valence-shell electrons. The contribution from the limit of the data to $E=\infty$ is estimated from extrapolation of a curve fitted to the higher energy measurements. This overall procedure makes use of the Thomas-Reiche-Kuhn (TRK) sum rule, which states that the dipole oscillator strength sum for an atom or molecule over all discrete transitions plus the integral over all continuum states is equal to the number of electrons N_e (e.g., 2 for helium). Thus

$$\left[\sum_m + \int_m\right] f^0_{0m} = N_e \ . \tag{16}$$

The TRK sum-rule normalization of a Bethe-Born converted EELS spectrum produces an accurate absolute scale without the need for the measurement of beam flux and target density required in conventional absolute cross-section determinations.

Direct selection of the conditions corresponding to the optical limit, together with TRK sum-rule normalization, provides an extremely direct and versatile approach, which is the basis of the dipole (e,e), $(e,2e)$, and $(e,e+\text{ion})$ techniques. These three methods provide quantitative simulations of tunable energy photoabsorption, photoelectron spectroscopy, and photoionization mass spectroscopy, respectively.[51,52,55] The three dipole electron-scattering techniques have been used extensively in recent years for total and partial optical oscillator strength measurements[55] in the continuum at modest energy resolution (1-eV FWHM) for a wide variety of valence-shell and inner-shell processes (see Refs. 53–59 for some recent examples). The modest energy resolution results from using an unmonochromated incident electron beam of thermal width. At such a low energy resolution the sharp peaks in the valence-shell excitation spectra of atoms and molecules are largely unresolved,[53–57] but the spectral envelope nevertheless encloses the correct integrated discrete oscillator strength, regardless of the bandwidth, since electron-impact excitation [Eq. (10)] is nonresonant.[27,51,52] This is in direct contrast to the situation for the (resonant) photoabsorption process [Eq. (9)] utilizing the Beer-Lambert law where line-saturation effects can cause drastic errors (see Sec. I C) in the discrete optical excitation oscillator strength spectrum.[29–33]

In view of the successful development and application[53–57] of low-resolution (LR) dipole (e,e) spectroscopy for quantitative valence-shell oscillator strength studies, and considering also the problems and limitations involved in the various direct optical techniques (particularly in the case of the Beer-Lambert law photoabsorption method, which is the only optical method that could even in principle be considered useful for general application), we now report the development and first application of a high-resolution (HR) dipole (e,e) method. This uses a high-impact-energy, 0° mean scattering angle, high-resolution EELS spectrometer of advanced design,[60] already developed for the study of valence- and inner-shell energy levels in this laboratory. The availability of very accurate quantum-mechanical calculations, together with the fact that helium has only a K shell and thus a total oscillator strength of exactly 2, with no corrections needed for Pauli excluded transitions,[61,62] makes the dipole excitation of ground-state helium an ideal test case for the HR dipole (e,e) method. In addition, further consistency checks can be made involving oscillator strength sums in appropriate regions of the discrete and continuum spectrum. In the present work test measurements, involving a completely independent determination of the absolute optical oscillator strengths for the $1\,^1S\rightarrow n\,^1P$ series ($n=2$–7) for helium, are compared with previously

published experimental data for $n=2-4$ obtained using a range of optical[12-20] and electron impact[39,47,63] methods. The measured results are also compared for $n=2-7$ with high-level quantum-mechanical calculations employing correlated wave functions.[3-10] The present measurements represent the first reported experimental results for $n=5-7$. Measurements of the absolute photoionization continuum oscillator strengths up to 180-eV photon energy, including the Fano profile resonance regions of double excitations around 60 and 70 eV, were also obtained and are compared with existing direct optical measurements[64-67] and calculations.[9,68-70] A preliminary communication of some of the results for discrete excitation has been published.[71] The results for helium are used to establish the viability of the HR dipole (e,e) method for general application to measurements of absolute optical oscillator strengths in the discrete valence-shell spectral regions of electronic excitation of atoms and molecules.

II. EXPERIMENTAL METHODS AND RESULTS

A. General procedures

The complementary performance characteristics of two different zero degree, high-impact-energy electron-energy-loss spectrometers, one with low resolution and known Bethe-Born factor and the other with very high energy resolution, were used to obtain the present experimental measurements of absolute optical oscillator strengths for the discrete photoexcitation and continuum photoionization of helium at high resolution. The combined techniques establish a general method suitable for routine application to measurements of absolute optical oscillator strengths for electronic excitation of atoms and molecules at high resolution over a wide spectral range. First, high-resolution electron excitation (energy loss) spectra of helium were obtained using a high-performance double hemispherical EELS spectrometer, for which the design and operational details have already been published.[60] This fully differentially pumped instrument has a high electron transmission at high energy resolution as a result of the advanced electron optical design and the large mean diameter (40 cm) of the hemispherical monochromator and analyzer. This spectrometer typically operates at an impact energy of 3000 eV, a mean scattering angle of 0°, and at an energy resolution selectable in the range 0.048–0.270 eV (FWHM). This instrument has been used extensively for measuring high-resolution valence-shell[72-74] and inner-shell[72,74-76] excitation spectra, but no attempt had been made thus far to make quantitative measurements of absolute oscillator strengths because the Bethe-Born factor of the spectrometer was not known until the presently reported work. In order to obtain absolute optical oscillator strengths from the high-resolution EELS spectra an absolute scale must be established and the energy-dependent Bethe-Born conversion factor for this spectrometer must be known with high precision. The conversion factor is in practice more complex than the expression shown in Eq. (15) because it must include integration over the finite spectrometer acceptance angles about $\theta=0°$. A sufficiently exact knowledge of the effective acceptance angles would require a very accurate and detailed understanding of the complex electron optical functions of the lenses in all regions of the high-resolution EELS spectrometer as a function of energy loss. Furthermore, this detailed information would be required for each analyzer-monochromator pass energy combination which must be selected to provide a given energy resolution. Such detailed information is difficult to obtain with sufficient precision by model calculations for the complex electron optics in this type of instrument. A better and more feasible approach is to calibrate the intensity response of the high-resolution instrument and obtain an empirically determined, relative Bethe-Born factor by referencing the high-resolution EELS signal to the known optical cross section in the smooth photoionization continuum spectral region of a suitable gas. This could be achieved by taking the ratio of the high-resolution EELS intensity to that of an independently measured absolute photoabsorption cross section, as a function of energy loss (photon energy). An obvious choice for this calibration is helium gas. Recommended experimental values of the absolute photoabsorption data for the helium continuum have been tabulated by Marr and West[77] from a consideration of a large number of published optical experiments. We have, however, chosen an alternative and entirely independent approach in which a high-sensitivity low-resolution (~1-eV FWHM) dipole (e,e) spectrometer, with no monochromator, simpler optics and collision geometry, and a well characterized Bethe-Born factor,[53-58] has been used to obtain a wide-range measurement of the helium discrete and continuum absolute photoabsorption oscillator strength, entirely independent of any optical measurement. This low-resolution dipole (e,e) spectrometer ($E_0=8000$ eV, $\theta=0°$, $\Delta\theta=1\times10^{-2}$ rad, $\Delta E=1.0$-eV FWHM) is the noncoincident forward-scattering portion of a dipole $(e,e+\text{ion})$ spectrometer that has been extensively used in this laboratory in recent years to obtain highly accurate photoabsorption and photoionization continuum total and partial oscillator strengths for a large number of molecular targets.[53-58] It has been found[55] that TRK sum-rule normalization of Bethe-Born converted EELS spectra obtained on this low-resolution dipole (e,e) spectrometer provides a highly accurate absolute photoabsorption oscillator strength scale, without the need for any measurement of beam flux or target density. Helium is a particularly suitable choice for the calibration measurements since it has only a single $(1s^2)$ shell and thus no shell separation or corrections for Pauli excluded transitions are required for the TRK sum-rule procedure, in contrast to the situation for more complex targets. The absolute photoabsorption oscillator strength obtained on the low-resolution dipole (e,e) spectrometer may then be used to generate the relative Bethe-Born factor for the high-resolution instrument by ratioing the signals in the smooth continuum region above the first ionization energy of helium, as described above. The relative Bethe-Born factor for the high-resolution spectrometer can then be obtained at lower energies by extrapolation of a suitable function fitted to the measured factor in the region above 25 eV. Finally, the

Bethe-Born converted high-resolution EELS spectrum of helium is placed on an absolute scale by single point normalization in the continuum (at 30 eV) to the absolute optical oscillator strength determined on the low-resolution dipole (e,e) instrument. With these procedures both the Bethe-Born calibration and the measurement of absolute optical oscillator strengths is achieved entirely independently of any optical techniques. Furthermore, exploitation of the TRK sum rule avoids the difficulties and limitations of conventional methods of absolute scale determination. The resulting absolute measurements can thus be independently compared with published values of measured and calculated optical oscillator strengths for helium. The sequence of measurements and procedures used in the present work are summarized by the flow chart shown in Fig. 6.

For quantitative measurements it is essential to ensure that saturated count rates are obtained in the channeltron detectors of both spectrometers over the full dynamic range of the signals. In order to avoid dead-time errors it was also necessary to use a fast data buffer between the output of the high-resolution spectrometer and the PDP 11/23 computer. Since for the high-resolution instrument no fast multichannel analyzer compatible with the computer was available, a specially adapted Nicolet 1073 signal averager was used as the data buffer in the present work. Maximum count rates were restricted to a maximum of 20 000 per second in order to ensure linearity over the full dynamic range of the spectra. Gas pressures were adjusted to be in the range $(0.5-2)\times10^{-5}$ Torr by means of a Granville-Phillips leak valve. Contributions from background gases remaining at the base pressure (2×10^{-7} Torr) of the turbomolecular pumped spectrometer were removed by subtracting the signal when the helium pressure was quartered. Such a procedure was used because complete removal of the sample gas was found to slightly influence the tuning of the energy-loss spectrometers.

B. Low-resolution optical oscillator strength measurements for helium

Using the low-resolution dipole (e,e) spectrometer, electron-energy-loss measurements were performed in the energy ranges 20–25.5, 25.5–50, 50–110, and 110–180 eV at intervals of 0.1, 0.5, 1, and 2 eV, respectively. The energy resolution was ~1-eV FWHM. Absolute optical oscillator strengths for helium were obtained by Bethe-Born conversion (using $\mathcal{C}_{LR}^{BB}$—see Fig. 6) and TRK sum-rule normalization (to a value of 2) of the electron-energy-loss data as described above. The portion of the relative oscillator strength from 180 eV to infinity was estimated from extrapolation of a least-squares fit to the data in the 72–180-eV region using a function of the form AE^{-B} (E is the energy and A and B are constants). The fit gives $B=2.5583$ and the fraction of the total oscillator strength above 180 eV was estimated to be only 4.65%. The helium $1\,^1S\rightarrow2\,^1P$ transition (21.218 eV) was used for calibration of the energy scale of the spectrum and is the only discrete structure resolved at the low resolution of this spectrometer. The measured data are recorded in Table I and illustrated in Fig. 7 (solid circles). Also shown in Fig. 7 are "recommended values" of the absolute photoabsorption (photoionization) data of helium (open triangles) as reported in the compilation by Marr and West.[77] The values compiled in Ref. 77 were obtained by Marr and West as follows: Various optical measurements of the photoionization cross section of helium in different energy ranges have been reported by different groups using optical methods.[78–80] West and Marr[81] have also themselves measured the photoionization of helium in the 340–40-Å (35–310-eV) range using synchrotron radiation. There are some slight discrepancies between the different data sets in some energy ranges. A critical evaluation of the various cross-section measurements was carried out[81] by giving a weight to the various data sets according to criteria such as the scatter of data points, performance, and quality of the monochromator used, etc. Then all the data were combined and the "best values" were obtained by fitting polynomials to the weighed data points. The resulting absolute photoionization cross-section data for helium and also for other noble gases in the vacuum uv and soft x-ray regions were then tabulated.[77]

It can be seen from Fig. 7 that the presently reported Bethe-Born converted, TRK sum-rule normalized, low-resolution dipole (e,e) results are in generally good quan-

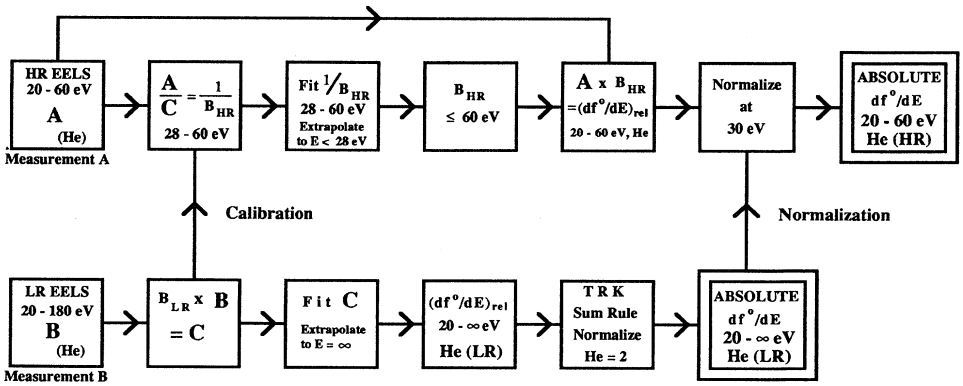

FIG. 6. Flow chart showing the data recording and processing procedures used in determining the absolute dipole oscillator strengths for the discrete electronic excitation transitions ($1\,^1S\rightarrow n\,^1P$, $n=2-7$) of helium.

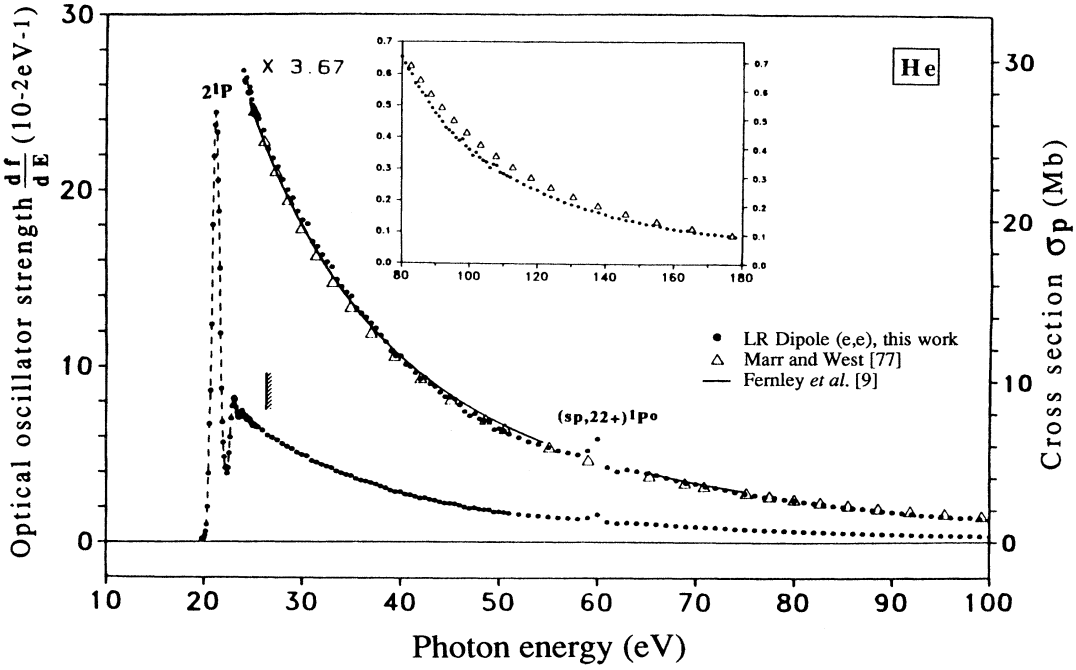

FIG. 7. Absolute dipole oscillator strengths for helium measured by the low-resolution dipole (e,e) spectrometer from 20–180 eV (FWHM = 1 eV). Solid circles are this work; open triangles are photoabsorption data of Marr and West (Ref. 77); solid line is theory, Fernley, Taylor, and Seaton (Ref. 9).

titative agreement with the absolute photoionization data recommended by Marr and West.[77] It should be noted that the two measuring techniques are physically different and also that the methods of obtaining the absolute scale are completely different. This provides convincing proof of the validity of the Bethe-Born theory and the quantitative equivalence of the dipole (e,e) and photoabsorption (photoionization) methods. In the region near 60 eV the dipole (e,e) data show evidence of the well-known double-excitation resonances of helium, whereas the Marr and West data[77] were simply obtained by fitting a smooth curve through the resonance region. Notwithstanding the excellent overall agreement, some small differences in shape are apparent. The Marr and West data[77] are slightly below and slightly above the present data in the 30–40 and 80–180-eV regions, respectively.

Also shown in Fig. 7 are the highly detailed photoionization cross-section calculations for helium recently reported by Fernley, Taylor, and Seaton[9] (solid line). The calculated data[9] have been shifted up in energy by 0.280 eV as the calculated first ionization energy of helium reported by Fernley, Taylor, and Seaton[9] is 0.280 eV lower than the accurately known spectroscopic value (24.59 eV). It can be seen that the calculations[9] are in excellent agreement with the present dipole (e,e) measurements. Similar calculations were reported earlier by Cooper[82] and by Bell and Kingston.[83]

The presently obtained low-resolution dipole (e,e) measurements (Table I, Fig. 7) have been used to obtain the Bethe-Born conversion factor ($\mathcal{C}^{BB}_{HR}$) for the high-resolution spectrometer and for normalization of the absolute scale (at 30 eV) by the methods described above (Sec. II A). The high-resolution results are presented in Sec. II C.

C. High-resolution optical oscillator strength measurements for helium

1. The discrete transitions $1\,^1S \rightarrow n\,^1P$ $(n=2-7)$

Using the high-resolution electron-energy-loss spectrometer, electron-energy-loss spectra of helium were obtained at an impact energy of 3000 eV in the energy-loss range 20–60 eV at a resolution of 0.048-eV FWHM and in the range 20–100 eV for resolutions of 0.072-, 0.098-, 0.155-, and 0.270-eV FWHM. The data have been processed using the procedures outlined in Sec. II A. The intensity of the high-resolution electron spectrum at each energy loss in the smooth continuum region above 25 eV was divided by the absolute optical oscillator strengths measured by the LR dipole (e,e) spectrometer (see Sec. II A, Table II, and Fig. 7). This quotient provides a relative Bethe-Born conversion factor ($\mathcal{C}^{BB}_{HR}$—see Fig. 6) for the high-resolution instrument in the energy range above 25 eV. In order to extend this Bethe-Born factor to the excitation region below 25 eV, the quotient has been fitted to a suitable function (which effectively represents the Bethe-Born correction factor for the HR spectrometer) over the energy range 28–60 eV and this function can then be extrapolated to lower energy. This fitting and the extrapolation must be done very carefully if correct experimental dipole oscillator strengths are then to be obtained in the discrete excitation region down to

21 eV for helium and to even lower energies (5 eV) for other atoms and molecules. In particular the effects of finite angular resolution about the forward-scattering direction must be properly accounted for in the Bethe-Born conversion factor if it is to be accurate over the long extrapolation down to 5 eV. Therefore the effects of angular resolution must be accounted for in some way in the fitting function.[51] In the real situation of finite acceptance angles it can be shown[51] that Eq. (15) at the optical limit can be modified to give

TABLE II. Absolute dipole oscillator strengths for helium obtained using the low-resolution dipole (e,e) spectrometer (24.6–180 eV).

Energy (eV)	Oscillator strength (10^{-2} eV^{-1})	Energy (eV)	Oscillator strength (10^{-2} eV^{-1})	Energy (eV)	Oscillator strength (10^{-2} eV^{-1})
24.6	7.05	46.5	2.04	94.0	0.421
24.7	6.96	47.0	1.97	95.0	0.412
24.8	6.85	47.5	2.00	96.0	0.397
24.9	6.76	48.0	1.92	97.0	0.388
25.0	6.62	48.5	1.90	98.0	0.393
25.1	6.71	49.0	1.89	99.0	0.370
25.2	6.66	49.5	1.75	100.0	0.360
25.3	6.58	50.0	1.77	101.0	0.341
25.4	6.58	51.0	1.68	102.0	0.350
25.5	6.55	52.0	1.63	103.0	0.335
26.0	6.37	53.0	1.56	104.0	0.326
26.5	6.08	54.0	1.52	105.0	0.321
27.0	5.94	55.0	1.48	106.0	0.302
27.5	5.81	56.0	1.43	107.0	0.314
28.0	5.61	57.0	1.40	108.0	0.310
28.5	5.45	58.0	1.37	109.0	0.288
29.0	5.33	59.0	1.43	110.0	0.284
29.5	5.12	60.0	1.61	112.0	0.273
30.0	4.98	61.0	1.18	114.0	0.262
30.5	4.92	62.0	1.11	116.0	0.250
31.0	4.65	63.0	1.14	118.0	0.240
31.5	4.57	64.0	1.11	120.0	0.232
32.0	4.45	65.0	1.08	122.0	0.219
32.5	4.34	66.0	1.05	124.0	0.211
33.0	4.26	67.0	1.01	126.0	0.204
33.5	4.07	68.0	0.968	128.0	0.194
34.0	3.95	69.0	0.926	130.0	0.187
34.5	3.87	70.0	0.912	132.0	0.181
35.0	3.81	71.0	0.869	134.0	0.173
35.5	3.63	72.0	0.850	136.0	0.168
36.0	3.55	73.0	0.822	138.0	0.162
36.5	3.49	74.0	0.785	140.0	0.155
37.0	3.40	75.0	0.757	142.0	0.147
37.5	3.32	76.0	0.735	144.0	0.144
38.0	3.21	77.0	0.708	146.0	0.138
38.5	3.11	78.0	0.698	148.0	0.136
39.0	2.97	79.0	0.669	150.0	0.130
39.5	2.89	80.0	0.652	152.0	0.125
40.0	2.90	81.0	0.632	154.0	0.123
40.5	2.76	82.0	0.612	156.0	0.118
41.0	2.73	83.0	0.598	158.0	0.112
41.5	2.63	84.0	0.569	160.0	0.109
42.0	2.54	85.0	0.557	162.0	0.106
42.5	2.56	86.0	0.540	164.0	0.106
43.0	2.46	87.0	0.529	168.0	0.0998
43.5	2.42	88.0	0.508	170.0	0.0980
44.0	2.33	89.0	0.491	172.0	0.0932
44.5	2.26	90.0	0.475	174.0	0.0916
45.0	2.25	91.0	0.464	176.0	0.0893
45.5	2.23	92.0	0.448	178.0	0.0856
46.0	2.14	93.0	0.429	180.0	0.0824

$$\frac{df^0(E)}{dE} = \left[\frac{EE_0}{\pi}\frac{\mathbf{k}_0}{\mathbf{k}_n}\right]\left[\ln\left[1+\frac{\theta_0^2}{x^2}\right]\right]^{-1}\frac{d^2\sigma_e(E)}{dEd\Omega}, \quad (17)$$

where $x=E/2E_0$ and θ° is the half-angle of acceptance emanating from the collision region as seen by the electron analyzer-detector system. At sufficiently high impact energy $\mathbf{k}_0 \sim \mathbf{k}_n$ and Eq. (17) can be rearranged to

$$F(E)=\frac{d^2\sigma_e(E)/dEd\Omega}{df^0(E)/dE}=\frac{a}{E}\ln\left[1+\frac{\theta_0^2}{x^2}\right]. \quad (18)$$

Thus we might expect a function of the form of the right-hand side of Eq. (18) to fit the ratio of the high-resolution electron-energy-loss spectrum to the absolute optical oscillator strength. While the use of Eq. (18) gave a quite reasonable fit, in practice a further improved fit to the ratio $F(E)$ in the continuum (28–60 eV) was obtained by adding an energy-dependent term to the constant a on the right-hand side of Eq. (18) to give

$$F(E)=\frac{d^2\sigma_e(E)/dEd\Omega}{df^0(E)/dE}=\frac{a+cE}{E}\ln\left[1+\frac{\theta_0^2}{x^2}\right]. \quad (19)$$

In this equation a and c are constants. $F(E)$ is equal to $1/\mathcal{C}_{\rm HR}^{\rm BB}$—see Fig. 6. Values of a, c, and θ_0 were determined from a least-squares best fit. The value of the half-angle θ_0 was found to be approximately 0.17°. At each resolution a function of this form fitted the data very well over the range 28–60 eV and was extrapolated to lower energies in order to convert $d^2\sigma_e(E)/dEd\Omega$ for discrete transitions in helium to a relative optical oscillator strength scale. The effectiveness of the extrapolation method employed has been examined by comparing the shapes of the photoabsorption oscillator strength curves down to 5 eV for a range of molecules (NO, N_2O, CO_2, and H_2O), obtained using the high-resolution dipole (e,e) method, with those obtained earlier using the low-resolution dipole (e,e) method and reported in a recent compilation by Gallagher *et al.*[55] The oscillator strength distribution in the two spectra for each molecule is consistent for energies down to 5 eV when the differences in energy resolution are considered. It should be noted that the exact form of $\mathcal{C}_{\rm HR}^{\rm BB}$ changes for the different resolution settings of the spectrometer. These $\mathcal{C}_{\rm HR}^{\rm BB}$ factors will be used for future oscillator strength measurements of other atoms and molecules.

The high-resolution energy loss spectra of helium were multiplied by the appropriate $\mathcal{C}_{\rm HR}^{\rm BB}$ function to obtain relative optical oscillator strength spectra, which were then normalized in the continuum region at 30 eV using the absolute data of Table II, as determined with the low-resolution spectrometer. A typical result at an energy resolution of 0.048 FWHM is shown in Fig. 8 which is the absolute optical oscillator strength spectrum of helium covering the range $n=2$–7 of the optically allowed discrete transitions ($1\,^1S \rightarrow n\,^1P$) preceding the first ionization threshold. Over the near threshold continuum region (24.6–30 eV) there is excellent quantitative agree-

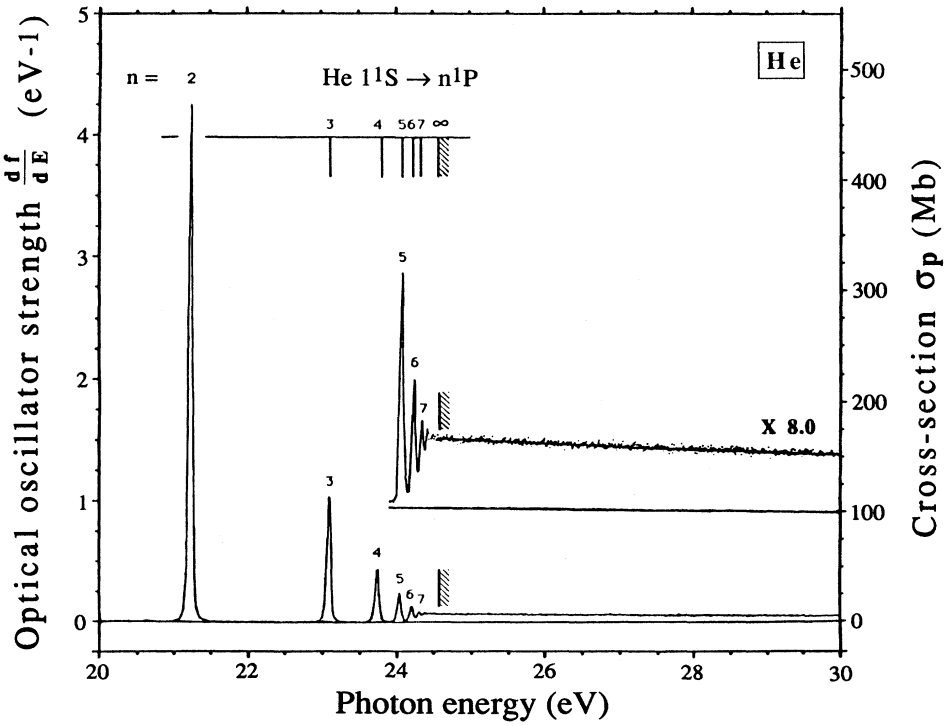

FIG. 8. Absolute dipole oscillator strengths for helium measured by the high-resolution electron-energy-loss spectrometer from 20–30 eV (FWHM=0.048 eV). Solid line above the ionization edge on ×8 spectrum is photoionization data from Marr and West (Ref. 77) and Fernley, Taylor, and Seaton (Ref. 9).

ment (see insert to Fig. 8) between the present work and the photoionization measurements compiled by Marr and West[77] and also the continuum calculations reported by Fernley, Taylor, and Seaton[9] (the data of Refs. 9 and 77 are represented by the solid line). Transitions up to $n=7$ for the $n\,^1P$ series are resolved. A very small peak barely visible at 20.6 eV represents a contribution from the dipole forbidden $1\,^1S\rightarrow 2\,^1S$ transition due to the finite (but very small) momentum transfer. This nondipole contribution is less than 0.5% of the $2\,^1P$ peak.

Integration of the peak areas in each spectrum, such as that in Fig. 8, provides a measure of the absolute oscillator strengths for each discrete transition in the $1\,^1S\rightarrow n\,^1P$ series. An analysis of the spectra obtained at a series of different energy resolutions results in the values shown in Table III. The uncertainties quoted represent the scatter in the measurements made at different resolutions. The absolute uncertainty is estimated to be ~5%. Other than the relative values for $n=3$ and 4 reported by De Jongh and Van Eck,[18] previously reported work (see Table III) has been confined to absolute values for $n=2$ and a few measurements[13,20,47,63] for $n=3$. The present data, which extend to $n=7$, represent the first measured values above $n=3$. Various other calculated and measured values for the helium $1\,^1S\rightarrow n\,^1P$ series are shown in Table III. Immediately it can be seen

TABLE III. (a) theoretical and (b) experimental determinations of the absolute dipole oscillator strengths for the ($1\,^1S\rightarrow n\,^1P$) transitions in helium. Estimated uncertainties in experimental measurements are shown in parentheses.

	Oscillator strength for transition from $1\,^1S$						Total to ionization threshold
	$2\,^1P$	$3\,^1P$	$4\,^1P$	$5\,^1P$	$6\,^1P$	$7\,^1P$	
		(a) Theory					
Fernley, Taylor, and Seaton (Ref. 9)	0.281 1	0.074 34	0.030 28	0.015 24	0.008 734	0.005 469	
Schiff, Pekeris, and Accad (Ref. 8)	0.276 2	0.073	0.030	0.015			
Weiss (Ref. 7)	0.276 0	0.073 2	0.030 3				
Green, Johnson, and Kolchin (Ref. 5)	0.275 62	0.072 94	0.029 59	0.014 84	0.008 461	0.05 25	
Dalgarno and Parkinson (Ref. 6)	0.276	0.073 4	0.029 9	0.015 1	0.008 6	0.005 4	0.424
Wiese, Smith, and Glennon (Ref. 10)	0.276 2	0.073 4	0.030 2	0.015 3	0.008 48	0.005 93	
Schiff and Pekeris (Ref. 4)	0.027 62	0.007 34					
Dalgarno and Stewart (Ref. 3)	0.270	0.074 6	0.030 4	0.015 3	0.008 78		
		(b) Experiment					
Present work [HR dipole (e,e)]	0.280	0.0741	0.0303	0.0152	0.008 92	0.005 87	0.431
	(0.007)	(0.0007)	(0.0007)	(0.0003)	(0.0005)	(0.0003)	(0.0006)
Tsurubuchi, Watanabe, and Arikawa (Ref. 20)	0.273	0.071					
(Self absorption)	(0.008)	(0.003)					
Westerveld and Van Eck (Ref. 19)	0.262						
(Self absorption)	(0.018)						
Backx *et al.* (Ref. 47)	0.276	0.073					0.421
(Electron impact)[a]							
Burger and Lurio (Ref. 13)	0.275	0.073					
(Lifetime: Level-crossing)	(0.007)	(0.005)					
DeJongh and Van Eck (Ref. 18)	0.276	0.076	0.029				
(Self absorption)[b]		(0.004)	(0.002)				
Lassettre, Skerbele, and Dillon (Ref. 30)	0.269						
(Electron impact)	(0.01)						
Martinson and Bickel (Ref. 14)	0.27						
(Lifetime: Beam foil)	(0.01)						
Fry and Williams (Ref. 12)	0.273						
(Lifetime: Hanle effect)	(0.011)						
Lincke and Griem (Ref. 15)	0.26						
(Plasmas emission profile)	(0.07)						
Korolyov and Odintsov (Ref. 16)	0.28						
(Beam emission profile)	(0.02)						
	0.26						
	(0.012)						
Kuhn and Vaughan (Ref. 17)	0.37						
(Resonance broadening	(0.03)						
emission profile)							
Geiger (Ref. 63)	0.312	0.0898					
(Electron impact)	(0.04)	(0.006)					

[a]Relative measurements normalized to the theoretical value for $n=2$ reported by Schiff and Pekeris (Ref. 4).
[b]Relative measurements normalized to the theoretical value for $n=2$ reported by Weiss (Ref. 7).

that the present high-resolution dipole (e,e) measurements are in excellent agreement across the range of n values with the calculations for helium reported by Schiff and Pekeris,[4] Fernley, Taylor, and Seaton,[9] and others[3,5–8,10] (see Table III). The earlier electron-impact measurements of Lassettre, Skerbele, and Dillon[39] for $n=2$ and of Backx *et al.*[47] for $n=3$, respectively, are reasonably consistent with the present more comprehensive work. The slightly lower value obtained for $n=2$ by Lassettre, Skerbele, and Dillon[39] may reflect the difficulties of extrapolation to $\mathbf{K}^2=0$ (see Sec. I D). The electron-impact data for $n=2$ and 3 reported by Geiger[63] show large departures from the present data and also from the calculations.[3–10] This could be partly due to the normalization procedure used by Geiger,[63] which was based on elastic scattering values, but as Lassettre, Skerbele, and Dillon[39] have pointed out, the ratio of the values for $n=2$ and 3 reported by Geiger shows a significant departure from the ratio of the calculated oscillator strength values.[3–10] The various optical mea-

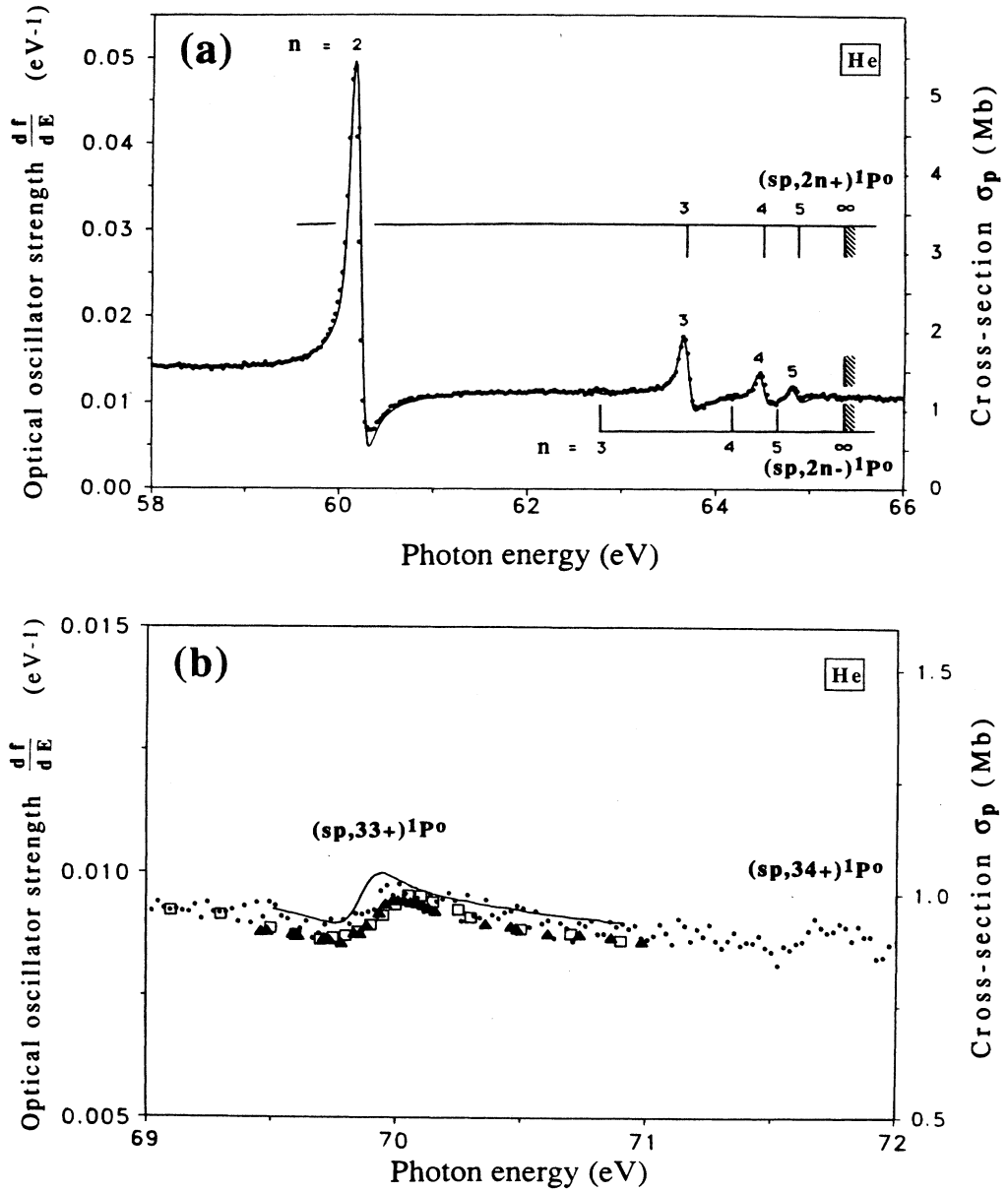

FIG. 9. Absolute dipole oscillator strengths for helium in the autoionizing resonance regions measured by the high-resolution electron-energy-loss spectrometer (a) in the energy region 58–66 eV—solid circles are this work; solid line is data from Fernley, Taylor, and Seaton (Ref. 9) (convoluted with the present experimental bandwidth of 0.115 eV); (b) in the energy region 69–72 eV—solid circles are this work; solid triangles are data of Kossmann, Krassig, and Schmidt (Ref. 67); open squares are data of Lindle *et al.* (Ref. 66); solid line is theory, Gersbacher and Broad (Ref. 69).

surements are in almost all cases restricted to $n=2$ (Refs. 12, 14–17, and 19) and in general are reasonably consistent with the present measurements and with theory.[3–10] The Hanle-effect measurement for $n=2$ reported by Fry and Williams[12] and the level crossing lifetime measurements reported for $n=2$ and 3 by Burger and Lurio[13] would seem to be the most accurate optical determinations. To the best of our knowledge, no Beer-Lambert law photoabsorption measurements have been reported for the helium discrete transitions, probably due to bandwidth difficulties or line-saturation effects discussed in Sec. I C. Such effects would be particularly difficult to avoid for the intense and extremely narrow lines in the helium resonance series. The self-absorption method used by De Jongh and Van Eck,[18] Westerveld and Van Eck,[19] and Tsurubuchi, Watanabe, and Arikawa[20] is not subject to line-saturation effects, but, unfortunately, like most other optical methods it is restricted in its application to the lower n values. A further interesting check on the presently reported data is the integrated oscillator strength for the discrete region up to the first ionization threshold. The value of 0.431 obtained in the present work is in good agreement with earlier estimates of 0.424,[6] 0.421,[47] and 0.427.[47]

2. *The autoionizing excited-state resonances*

The energies and profiles of the well-known autoionizing doubly excited resonances of helium in the 59–72-eV energy region have been previously studied in some detail both experimentally[64–67,84] and theoretically.[68–70,85] In the present work, this region containing the autoionizing resonances was remeasured with the use of the HR dipole (e,e) spectrometer at medium resolution. By dividing the HR electron-energy-loss spectrum at each energy loss in the smooth regions of the continuum by the absolute optical oscillator strength measured by the LR dipole (e,e) spectrometer (see Sec. II A, Table II, and figure 7) values of $\mathcal{C}_{\mathrm{HR}}^{\mathrm{BB}}$ in the energy region of the autoionizing resonances were obtained. A fitted curve through these points permitted interpolated values of $\mathcal{C}_{\mathrm{HR}}^{\mathrm{BB}}$ to be obtained in a continuous form throughout the resonance region. The Bethe-Born converted relative optical oscillator strength spectrum was normalized in the smooth continuum region at 75 eV using the absolute photoabsorption oscillator strength data from Table II, as determined by the LR dipole (e,e) spectrometer. The present results for the absolute optical oscillator strengths throughout the region of the autoionizing doubly-excited-state resonances below the $He^+(2s)$ and $He^+(3s)$ thresholds are shown in Figs. 9(a) and 9(b), respectively.

In Fig. 9(a) the absolute oscillator strengths for the autoionizing resonances below the $He^+(2s)$ threshold calculated by Fernley, Taylor, and Seaton[9] (solid line) are convoluted with the present experimental Gaussian-shaped energy bandwidth of 0.115 eV. The energy scale of the data calculated by Fernley, Taylor, and Seaton[9] has been shifted by +0.280 eV to give a correct energy scale (see Sec. II A). It can be seen that there is generally excellent agreement in both the shapes and magnitudes of the resonances between the calculations of Fernley, Taylor, and Seaton[9] (solid line) and the present experimental work (dots), except for the minimum of the $(sp,22+)\ ^1P^\circ$ state. Slight differences in the energies of the maxima of the resonances are also observed. The energies of the maxima of the $(sp,2n+)\ ^1P^\circ$ resonances for $n=2$–5 have been determined in the present work to be 60.150, 63,655, 64.465, and 64.820 eV, respectively. These values are in good agreement with those reported earlier.[64,65,67,68,70]

The autoionizing resonances $(sp,33+)$ and $(sp,34)\ ^1P^\circ$ were also observed in the present work. In Fig. 9(b), the present data (dots) are compared with other experimental results by Lindle *et al.*[66] (open squares) and by Kossmann, Krassig, and Schmidt[67] (solid triangles), who normalized their results at 68.9 eV using the Marr and West tabulated data.[77] The solid line in Fig. 9(b) represents theoretical values calculated by Gerbachber and Broad.[69]

III. CONCLUSIONS

The present high-resolution dipole (e,e) measurements of optical oscillator strengths for the discrete excitation transitions $(1\ ^1S\rightarrow n\ ^1P,\ n=2$–$7)$, the autoionizing doubly-excited-state resonances and also the photoionization continuum have considerably extended the range of measured absolute oscillator strength data for helium. The presently reported results are all in excellent quantitative agreement with sophisticated quantum-mechanical calculations carried out using correlated wave functions[4–9] and are consistent with most optical and other measurements for those few transitions where such experimental data were previously available. These findings confirm the validity of the Bethe-Born approximation and the suitability of the high resolution dipole (e,e) method using TRK sum-rule normalization for general application to the measurement of optical oscillator strengths for discrete electronic excitations in atoms and molecules at high resolution. The dipole (e,e) method provides a ready means of oscillator strength measurement across the entire valence shell region at high resolution and does not suffer from the problems of line-saturation bandwidth effects that can complicate Beer-Lambert law photoabsorption studies. The high-resolution dipole (e,e) method is now being applied to the measurement of absolute optical oscillator strengths for electronic excitation of other atoms as well as diatomic and small polyatomic molecules.

ACKNOWLEDGMENTS

This work has been financially supported by the Natural Sciences and Engineering Research Council of Canada. One of us (W.F.C.) gratefully acknowledges support from the University of British Columbia (UBC). We would like to thank B. Greene, D. Jones, and M. Hatton (Electronics shop, Department of Chemistry, UBC) for assistance with the maintenance of the dipole (e,e) spectrometers and with the design and construction of the fast data buffer. We would also like to thank Professor M. J. Seaton for sending us his calculated data and helpful comments concerning this work. Helpful discussions with Dr. W. L. Wiese and Dr. M. Inokuti are also acknowledged.

[1]*Proceedings of Workshop on Electronic and Ionic Collision Cross Sections Needed in the Modeling of Radiation Interactions with Matter, Argonne, Illinois, 1983* (Argonne National Laboratory, Argonne, 1984), Report No. ANL-84-28.
[2]L. C. Green, P. P. Rush, and C. D. Chandler, Astrophys. J. Suppl. Ser. **3**, 37 (1957).
[3]A. Dalgarno and A. L. Stewart, Proc. Phys. Soc. London **76**, 49 (1960).
[4]B. Schiff and C. L. Pekeris, Phys. Rev. A **134**, 638 (1964).
[5]L. C. Green, N. C. Johnson, and E. K. Kolchin, Astrophys. J. **144**, 369 (1967).
[6]A. Dalgarno and E. M. Parkinson, Proc. R. Soc. London Ser. A **301**, 253 (1967).
[7]A. W. Weiss, J. Res. Natl. Bur. Stand. **71A**, 163 (1967).
[8]B. Schiff, C. L. Pekeris, and Y. Accad. Phys. Rev. A **4**, 885 (1971).
[9] J. A. Fernley, K. T. Taylor, and M. J. Seaton, J. Phys. B **20**, 6457 (1987).
[10]W. L. Wiese, M. W. Smith, and B. M. Glenon, Atomic Transition Probabilities: Hydrogen through Neon, Natl. Stand. Ref. Data Ser., Natl. Bur. Stand. (U.S.) Circ. No. 4 (U.S. GPO, Washington, DC, 1966), Vol. I; W. L. Wiese, M. W. Smith, and B. M. Miles, Atomic Transition Probabilities: Sodium through Calcium, *ibid.*, Circ. No. 22, (U.S. GPO, Washington, DC, 1969), Vol. II; G. A. Martin, J. R. Fuhr, and W. L. Wiese, Atomic Transition Probabilities: Scandium through Manganese, J. Phys. Chem. Ref. Data **17**, Suppl. 3 (1988); J. R. Fuhr, G. A. Martin, and W. L. Wiese, Atomic Transition Probabilities: Iron through Nickel, *ibid.* **17**, Suppl. 4 (1988).
[11]K. Yoshino, D. E. Freeman, J. R. Esmond, R. S. Friedman, and W. H. Pakinson, Planet. Space Sci. **36**, 1201 (1988).
[12]E. S. Fry and W. L. Williams, Phys. Rev. **183**, 81 (1969).
[13]J. M. Burger and A. Lurio, Phys. Rev. A **3**, 64 (1971).
[14]I. Martinson and W. S. Bickel, Phys. Lett. **30A**, 524 (1969).
[15]R. Lincke and H. R. Griem, Phys. Rev. **143**, 66 (1966).
[16]F. A. Korolyov and V. I. Odintsov, Opt. Spectrosc. **18**, 547 (1965).
[17]H. G. Kuhn and J. M. Vaughan, Proc. R. Soc. London Ser. A **277**, 297 (1964).
[18]J. P. De Jongh and J. Van Eck, Physica **51**, 104 (1971).
[19]W. B. Westerveld and J. Van Eck, J. Quant. Spectrosc. Radiat. Transfer **17**, 131 (1977).
[20]S. Tsurubuchi, K. Watanabe, and T. Arikawa, J. Phys. B **22**, 2969 (1989).
[21]Y. M. Aleksandrov, P. F. Gruzdev, M. G. Kozlov, A. V. Loginov, R. V. Fedorchuk, and M. N. Yakimenko, Opt. Spectrosc. **54**, 4 (1983).
[22]W. R. Ferrell, M. G. Payne, and W. R. Garrett, Phys. Rev. A **35**, 5020 (1987).
[23]S. Brodersen, J. Opt. Soc. Am. **44**, 22 (1954).
[24]G. F. Lothian, Analyst **88**, 678 (1963).
[25]R. D. Hudson and V. L. Carter, J. Opt. Soc. Am. **58**, 227 (1968).
[26]R. D. Hudson, Rev. Geophys. Space Phys. **6**, 305 (1971).
[27]M. Inokuti, Rev. Mod. Phys. **43**, 297 (1971).
[28]J. W. C. Johns, W. A. Kreiner, and J. Susskind, J. Mol. Spectrosc. **60**, 400 (1976).
[29]G. R. Cook and P. H. Metzger, J. Chem. Phys. **41**, 321 (1964).
[30]R. E. Huffman, Y. Tananka, and J. C. Larrabee, J. Chem. Phys. **39**, 910 (1963).
[31]G. M. Lawrence, D. L. Mickey, and K. Dressler, J. Chem. Phys. **48**, 1989 (1968).
[32]V. L. Carter, J. Chem. Phys. **56**, 4195 (1972).
[33]P. Gürtler, V. Saile, and E. E. Koch, Chem. Phys. Lett. **48**, 245 (1977).
[34]R. N. S. Sodhi and C. E. Brion (unpublished).
[35]E. N. Lassettre, F. M. Glaser, V. D. Meyer, and A. Skerbele, J. Chem. Phys. **42**, 3429 (1965).
[36]J. Geiger and W. Stickel, J. Chem. Phys. **43**, 4535 (1965).
[37]H. Bethe, Ann. Phys. (Leipzig) **5**, 325 (1930).
[38]E. N. Lassettre, A. Skerbele, and M. A. Dillon, J. Chem. Phys. **50**, 1829 (1969).
[39]E. N. Lassettre, A. Skerbele, and M. A. Dillon, J. Chem. Phys. **52**, 2797 (1970).
[40]E. N. Lassettre and A. Skerbele, J. Chem. Phys. **54**, 1597 (1971).
[41]A. Skerbele and E. N. Lassettre, J. Chem. Phys. **55**, 424 (1971).
[42]I. V. Hertel and K. J. Ross, J. Phys. B **2**, 285 (1969).
[43]M. J. Van der Wiel, Physica **49**, 411 (1970).
[44]M. J. Van der Wiel and G. Wiebes, Physica **53**, 225 (1971).
[45]M. J. Van der Wiel and G. Wiebes, Physica **54**, 411 (1971).
[46]M. J. Van der Wiel and C. E. Brion, J. Electron Spectrosc. Relat. Phenom. **1**, 443 (1972/73).
[47]C. Backx, R. R. Tol, G. R. Wight, and M. J. Van der Wiel, J. Phys. B **8**, 2050 (1975).
[48]C. Backx, G. R. Wight, and M. J. Van der Wiel, J. Phys. B **9**, 315 (1976).
[49]G. R. Wight, M. J. Van der Wiel, and C. E. Brion, J. Phys. B **9**, 675 (1976).
[50]A. Hamnett, W. Stoll, G. R. Branton, C. E. Brion, and M. J. Van der Wiel, J. Phys. B **9**, 945 (1976).
[51]C. E. Brion and A. Hamnett, Advan. Chem. Phys. **45**, 1 (1981).
[52]C. E. Brion, Comments At. Mol. Phys. **16**, 249 (1985).
[53]Y. Iida, F. Carnovale, S. Daviel, and C. E. Brion, Chem. Phys. **105**, 211 (1986).
[54]W. Zhang, G. Cooper, T. Ibuki, and C. E. Brion, Chem. Phys. **137**, 391 (1989).
[55]J. W. Gallagher, C. E. Brion, J. A. R. Samson, and P. W. Langhoff, J. Phys. Chem. Ref. Data **17**, 9 (1988).
[56]G. Cooper, T. Ibuki, and C. E. Brion, Chem. Phys. **140**, 133 (1990).
[57]E. B. Zarate, G. Cooper, and C. E. Brion, Chem. Phys. **148**, 277 (1990).
[58]G. Cooper, T. Ibuki, and C. E. Brion, Chem. Phys. **140**, 147 (1990).
[59]E. B. Zarate, G. Cooper, and C. E. Brion, Chem. Phys. **148**, 289 (1990).
[60]S. Daviel, C. E. Brion and A. P. Hitchcock, Rev. Sci. Instrum. **55**, 182 (1984).
[61]J. A. Wheeler and J. A. Bearden, Phys. Rev. **46**, 755 (1934).
[62]J. L. Dehmer, M. Inokuti, and R. P. Saxon, Phys. Rev. A **12**, 102 (1975).
[63]J. Geiger, Z. Phys. **175**, 530 (1963).
[64]R. P. Madden and K. Codling, Astrophys. J. **141**, 364 (1965).
[65]H. D. Morgan and D. L. Ederer, Phys. Rev. A **29**, 1901 (1984).
[66]D. W. Lindle, T. A. Ferrett, P. A. Heimann, and D. A. Shirley, Phys. Rev. A **36**, 2112 (1987).
[67]H. Kossmann, B. Krassig, and V. Schmidt, J. Phys. B **21**, 1489 (1988).
[68]D. H. Oza, Phys. Rev. A **33**, 824 (1986).
[69]R. Gersbacher and T. T. Broad, J. Phys. B **23**, 365 (1990).
[70]C. F. Fischer and M. Idrees, J. Phys. B **23**, 679 (1990).
[71]W. F. Chan, G. Cooper, K. H. Sze, and C. E. Brion, J. Phys. B

23, L523 (1990).
[72]K. H. Sze, C. E. Brion, M. Tronc, S. Bodeur, and A. P. Hitchcock, Chem. Phys. **121**, 279 (1988).
[73]K. H. Sze, C. E. Brion, A. Katrib, and B. El-Issa, Chem. Phys. **137**, 369 (1989).
[74]G. Cooper, K. H. Sze, and C. E. Brion, J. Am. Chem. Soc. **111**, 5051 (1989).
[75]K. H. Sze, C. E. Brion, and A. Katrib, Chem. Phys. **132**, 271 (1989).
[76]W. Zhang, K. H. Sze, C. E. Brion, X. M. Tong, and T. M. Li, Chem. Phys. **140**, 265 (1990).
[77]G. V. Marr and J. B. West, At. Data Nucl. Data Tables **18**, 497 (1976).
[78]J. F. Lowry, D. H. Tomboulian, and D. L. Ederer, Phys. Rev. A **137**, 1054 (1965).
[79]J. A. R. Samson, *Advances in Atomic and Molecular Physics* (Academic, New York, 1966), Vol. 2, p. 177.
[80]W. S. Watson, J. Phys. B **5**, 2292 (1972).
[81]J. B. West and G. V. Marr, Proc. R. Soc. London Ser. A **349**, 397 (1976).
[82]J. W. Cooper, Phys. Rev. **128**, 681 (1962).
[83]K. L. Bell and A. E. Kingston, Proc. Phys. Soc. London **90**, 31 (1967).
[84]S. M. Silverman and E. N. Lassettre, J. Chem. Phys. **40**, 1265 (1964).
[85]U. Fano, Phys. Rev. **124**, 1866 (1961).
[86]W. F. Chan, G. Cooper, and C. E. Brion (unpublished).